THE ASTROPHYSICAL JOURNAL, 257:125–134, 1982 June 1

MEASUREMENTS OF CH AND CH^+ IN DIFFUSE INTERSTELLAR CLOUDS

S. R. FEDERMAN
Department of Astronomy, and McDonald Observatory, University of Texas at Austin
Received 1981 September 28; accepted 1981 December 11

ABSTRACT

A survey of CH and CH^+ absorption was made for directions with known amounts of atomic and molecular hydrogen. Both radicals are detected only toward directions with substantial amounts of H_2 [$N(H_2) \gtrsim 10^{18}$ cm^{-2}]. The column density of CH varies linearly with $N(H_2)$; $N(CH^+)$ is independent of $N(H_2)$. The CH line is shifted in velocity from the CH^+ line in $\sim 50\%$ of the lines of sight. A model which incorporates the presence of a shock best describes the chemical and the dynamical information available from the data.

Subject headings: interstellar: abundances — interstellar: molecules

I. INTRODUCTION

Chemical models have been formulated in an attempt to understand the abundances of CH and CH^+ in diffuse interstellar clouds. In the belief that diffuse clouds are predominantly H I, Bates and Spitzer (1951) and Solomon and Klemperer (1972) proposed that CH and CH^+ are produced and are destroyed through chemical reactions involving atomic species, electrons, and the ambient radiation field. Results from the *Copernicus* satellite, however, indicate that molecular hydrogen is a major constituent of diffuse clouds (e.g., Savage *et al.* 1977). This fact led Black and Dalgarno (1973) and Black, Dalgarno, and Oppenheimer (1975) to consider reactions involving H_2 also. When Mitchell and McGowen (1978) found the dissociative recombination of CH^+ to be rapid, all the above chemical models failed to reproduce the limited number of observed abundances available for CH *and* CH^+. The presence of a shock modifies the chemistry for carbon hydrides (Elitzur and Watson 1978, 1980): a reaction for producing CH^+ which is endothermic at 80 K (the ambient temperature of the gas) proceeds in the hot postshock region; the production of CH takes place in the cold postshock gas farther downstream via reactions elucidated by Black and Dalgarno (1973).

A comprehensive survey of CH and CH^+ in absorption toward lines of sight with and without a substantial amount of H_2 can discriminate among the various gas phase chemical models through the trends seen in the data. For example, if atomic hydrogen is important in forming carbon hydrides, a linear relationship between carbon hydrides and atomic hydrogen would be expected (Jura and Smith 1977). Conversely, a correlation between carbon hydride and molecular hydrogen would indicate the importance of H_2 in the chemistry. A shift in the velocity of the line centers for CH and CH^+ toward a specific direction would suggest the presence of a shock. The results from *Copernicus* for H I (Bohlin, Savage, and Drake 1978) and for H_2 (Savage *et al.* 1977) are used as a guide for lines of sight to study. Observations of CH λ4300 and CH^+ λ4232 with high spectral resolution and high sensitivity were made in order to apply the tests described above. The present work complements previous studies (Frisch 1972; Cohen 1973; Hobbs 1973; and Chaffee 1974, 1975) because the chemical models used to analyze the previous data have since been modified and refined. Emphasis in the present work is placed on lines of sight not previously studied, but for some lines of sight, the CH and CH^+ lines were re-observed to obtain higher precision.

Results from the present survey for the lines of sight toward the Perseus OB2 association and toward the Pleiades already have been published (Federman 1980, 1982). For these two directions, evidence for a shock is found. Evidence for a shock toward the Sco OB2 association and consequences of the shock are discussed in Meyers *et al.* (1982). The complete set of data is presented here to search for any additional systematic trends.

II. DATA

Measurements of the 4300.321 Å line for CH and the 4232.539 Å line for CH^+ were made between 1979 September and 1981 June. The spectra were obtained with the Reticon photodiode array on the coudé spectrograph of the 2.7 m telescope at McDonald Observatory (Vogt, Tull, and Kelton 1978). An echelle grating, with 79 rulings per mm, in 53rd and 54th order for the CH and CH^+ line, respectively, was used to give dispersions of 0.653 Å mm^{-1} and 0.636 Å mm^{-1}, respectively. The entrance slit to the spectrograph was set either to 220 or 440 μm, corresponding to a spectral resolution of either 2.2 or 4.4 km s^{-1} at 4300 Å. The lines were fully resolved even with the larger slit. The larger slit was used in the majority of cases, thus allowing more light to enter the spectrograph. Each spectrum was exposed for a sufficient time to ensure a signal-to-noise ratio in the continuum in excess of 100.

Special care was required to obtain precise line velocities for the present observations. Any effects of an S-curve in the photodiode array were eliminated by placing the absorption lines at the same position on the array. The accuracy of the velocity scale was tested by

taking an Fe/Ne calibration spectrum; the spectrograph was stable to within 1.1 km s^{-1} (one diode). Contamination from the stellar spectra was minimal; only for several late B stars did the Fe II line near 4232 Å appear in the spectrum. The high rotational velocity of the stars easily discriminated between stellar Fe II and interstellar CH^+.

The data first were reduced with a program which produced flat continua. The program also removed the remaining fixed pattern noise of the Reticon array, which was not divided out from the continuum by the Reticon software package (Vogt *et al.*). The root mean square error in the continuum was determined over an interval of 50 diodes. The interstellar lines measured here typically covered 12 diodes; upper limits to absorption lines were set at the 2 σ limit based on the error in the continuum. If a line was detected, the core of the line was fitted by a Gaussian profile with a least-squares program. The fitting procedure yielded the velocity at line center v_{LSR} and the Doppler parameter b. The Gaussian profile did

TABLE 1

CH AND CH^+ MEASUREMENTS

STAR		CH		CH^+				
HD No.	Name	W_λ (mÅ)	N (cm^{-2})	W_λ (mÅ)	N (cm^{-2})	N(H I) (cm^{-2})	$N(H_2)$ (cm^{-2})	NOTES
886	γ Peg	...	...	<1.4	<1.2(12)	1.1(20)	<1.6(14)	
2905	κ Cas	6.9 ± 2.0	8.0(12)	4.1 ± 1.5	3.6(12)	1.6(21)	1.9(20)	a, b
5394	γ Cas	...	...	<1.5	<1.3(12)	1.4(20)	<3.2(17)	
21278	...	...	...	4.1 ± 1.9	3.6(12)	...	3.0(19)	
22928	δ Per	...	...	<1.5	<1.3(12)	...	2.0(19)	
23180	o Per	11.2 ± 4.9	1.3(13)	5.1 ± 2.7	4.5(12)	7.9(20)	4.1(20)	
23408	20 Tau	1.3 ± 0.5	1.5(12)	20.2 ± 1.8	1.8(13)	...	5.6(19)	
23480	23 Tau	<2.9	<3.3(12)	12.5 ± 2.2	1.1(13)	...	1.3(20)	
23630	η Tau	<1.8	<2.1(12)	1.6 ± 0.4	1.4(12)	...	3.5(19)	
24398	ζ Per	15.9 ± 2.9	1.8(13)	2.6 ± 0.9	2.3(12)	6.5(20)	4.7(20)	
24760	ϵ Per	<1.7	<2.0(12)	<0.9	<7.9(11)	2.5(20)	3.4(19)	
24912	ξ Per	9.4 ± 3.3	1.1(13)	17.8 ± 2.1	1.6(13)	1.3(21)	3.4(20)	b
30614	α Cam	5.6 ± 2.2	6.5(12)	15.7 ± 1.8	1.4(13)	7.9(20)	2.2(20)	
35149	23 Ori	...	...	10.1 ± 1.5	8.8(12)	5.5(20)	1.0(18)	
36486	δ Ori	...	...	<1.6	<1.4(12)	1.7(20)	4.8(14)	
36861	λ Ori	...	...	<1.5	<1.3(12)	6.0(20)	1.3(19)	
37022	θ^1 Ori C	...	...	<3.7	<3.2(12)	1.1(21)	<3.5(17)	
37043	ι Ori	...	...	<1.2	<1.1(12)	1.4(20)	4.9(14)	
37128	ϵ Ori	...	...	<1.0	<8.8(11)	2.8(20)	3.7(16)	
37202	ζ Tau	...	...	<2.2	<1.9(12)	1.1(20)	<4.7(17)	
37742	ζ Ori	...	...	<0.8	<7.0(11)	2.6(20)	5.4(15)	
38771	κ Ori	...	...	<1.6	<1.4(12)	3.3(20)	4.8(15)	
44743	β CMa	...	...	<1.2	<1.1(12)	<5.0(18)	<2.0(17)	
47839	15 Mon	...	...	<3.6	<3.2(12)	2.5(20)	3.5(15)	
		...	...	<3.4	<3.0(12)			
87901	α Leo	...	...	<0.9	<7.9(11)	...	<9.5(14)	
91316	ρ Leo	...	...	<1.1	<9.6(11)	1.8(20)	4.1(15)	
116658	α Vir	...	...	<0.8	<7.0(11)	<1.0(19)	5.6(12)	
120315	η UMa	...	...	<0.7	<6.1(11)	...	2.4(13)	
135742	β Lib	...	...	<1.3	<1.1(12)	...	2.2(14)	
143018	π Sco	...	...	<2.0	<1.8(12)	5.2(20)	2.1(19)	
143275	δ Sco	...	...	2.5 ± 0.6	2.2(12)	1.4(21)	2.6(19)	
144217 A	β^1 Sco	3.5 ± 1.3	4.0(12)	3.9 ± 1.1	3.4(12)	1.2(21)	6.8(19)	
144470	ω^1 Sco	3.0 ± 1.5	3.5(12)	4.1 ± 1.6	3.6(12)	1.5(21)	1.1(20)	
145502	ν Sco AB	2.8 ± 1.2	3.2(12)	3.4 ± 1.4	3.0(12)	1.4(21)	7.8(19)	
147165	σ Sco	3.9 ± 1.6	4.5(12)	6.8 ± 2.5	6.0(12)	2.2(21)	6.2(19)	
164353	67 Oph	3.8 ± 1.9	4.4(12)	5.9 ± 1.3	5.2(12)	1.0(21)	1.8(20)	a
167264	15 Sgr	...	...	4.7 ± 1.7	4.1(12)	1.4(21)	1.9(20)	
175191	σ Sgr	...	...	<1.5	<1.3(12)	<3.0(19)	<1.0(14)	
184915	κ Aql	7.6 ± 2.3	8.8(12)	4.6 ± 1.1	4.0(12)	7.9(20)	2.0(20)	
200120	59 Cyg	...	...	<3.0	<2.6(12)	1.8(20)	2.1(19)	
		...	...	<3.4	<3.0(12)			
203064	68 Cyg	7.0 ± 2.2	8.1(12)	4.4 ± 1.8	3.8(12)	1.0(21)	1.9(20)	
214680	10 Lac	...	...	<2.6	<2.3(12)	5.0(20)	1.7(19)	
217675	o And	<1.1	<1.3(12)	<0.8	<7.0(11)	...	4.7(19)	
218376	1 Cas	6.6 ± 3.1	7.6(12)	9.4	8.2(12)	8.9(20)	1.4(20)	a, c
224572	σ Cas	3.0 ± 1.6	3.5(12)	6.4 ± 1.7	5.6(12)	7.6(20)	1.7(20)	a, b

[a] Possibly two CH^+ components.
[b] Possibly two CH components.
[c] CH^+ from Hobbs 1973.

not reproduce the wings of the lines well; therefore, the equivalent widths W_λ were measured with a planimeter.

Table 1 lists the equivalent width and the derived column density measured for each of the lines of sight. The data include 12 new detections of CH and 11 new detections of CH$^+$. Representative spectra are shown in Figures 6–8. The quoted 1 σ error for W_λ is the root mean square error in the continuum over the extent of the line wings. As mentioned above, upper limits are set at 2 σ. The lines are weak; the optical depth in the center of the line is sufficiently small (<0.3) to ensure that the column density N is proportional to W_λ. The oscillator strength is needed to derive the proportionality constant. Brzozowski *et al.* (1976) made lifetime measurements of CH at high resolution that distinguished individual rotational and vibrational states. Their results agree with previous measurements (Fink and Welge 1967; Linevsky 1967; Hesser and Lutz 1970), indicating that an oscillator strength of 5.3×10^{-3} for the $A\ ^2\Delta$–$X\ ^2\Pi$ transition of CH is appropriate. When electrostatic repulsion effects in measurements using the phase-shift technique are properly taken into account, Erman (1977) found that the oscillator strength for the $A\ ^1\Pi$–$X\ ^1\Sigma$ transition of CH$^+$ is 7.2×10^{-3}. The relationships between N and W_λ using the above oscillator strengths are:

$$N(\mathrm{CH}) = 1.15 \times 10^{12}[W_\lambda(\mathrm{CH})/\mathrm{m\AA}]\ \mathrm{cm}^{-2}$$

and

$$N(\mathrm{CH}^+) = 8.76 \times 10^{11}[W_\lambda(\mathrm{CH}^+)/\mathrm{m\AA}]\ \mathrm{cm}^{-2}\ .$$

[Recently, Mahan and O'Keefe (1981) measured in an ion trap the oscillator strength for the CH$^+$ transition and found $f = 5.6 \times 10^{-3}$. Their result is independent of electrostatic repulsion and thus probably is the best estimate for f. Use of their oscillator strength increases $N(\mathrm{CH}^+)$ by $\sim 30\%$, but since all the determinations of $N(\mathrm{CH}^+)$ are increased by the same factor, the trends seen in Figs. 1*b*, 3, and 4 are unaltered.]

The velocity at line center and the Doppler parameter are shown in Table 2. To extract the Doppler parameter from the width determined by the Gaussian fit, the resolution of the spectrograph was considered. The 1 σ errors for both v_{LSR} and b were determined by the least-squares fitting procedure without incorporating systematic effects such as a drift in the velocity scale.

The data are displayed graphically in Figures 1–4. The filled circles represent the results of the present work, while open circles are the results of other researchers for additional lines of sight. The sources for the additional data are Frisch (1972) for HD 193322, Hobbs (1973) for ϕ Per and 1 Cas, Chaffee (1975) for ρ Oph A and ζ Oph, Jura and Smith (1977) for τ Sco, Chaffee and Dunham (1979) for stars in Cepheus, and Frisch (1979) for χ Oph. The CH$^+$ results for 15 Mon, 59 Cyg, 1 Cas, and σ Cas are not plotted because of the uncertainty of attributing the H I or the H_2 to a specific velocity component. Arrows indicate limiting values for the column densities. Figure 1 shows N(CH) and $N(\mathrm{CH}^+)$ plotted against N(H I). The dashed line has a slope of unity and is used for comparison with chemical models

TABLE 2

LINE PARAMETERS

Star		CH		CH$^+$	
HD No.	Name	V_{LSR} (km s^{-1})	b (km s^{-1})	V_{LSR} (km s^{-1})	b (km s^{-1})
2905	κ Cas	-10.7 ± 0.4	3.5 ± 0.6	-12.7 ± 0.5	1.8 ± 0.4
21278	...	...	...	$+4.0 \pm 0.6$	2.6 ± 0.8
23180	o Per	$+7.7 \pm 0.4$	2.5 ± 0.5	$+6.1 \pm 0.1$	2.0 ± 0.2
23408	20 Tau	$+8.3 \pm 0.7$	1.5 ± 0.7	$+11.5 \pm 0.1$	2.2 ± 0.1
23480	23 Tau	...	...	$+9.8 \pm 0.2$	2.8 ± 0.2
23630	η Tau	...	...	$+8.2 \pm 0.2$	1.9 ± 0.2
24398	ζ Per	$+8.1 \pm 0.1$	1.9 ± 0.1	$+7.7 \pm 0.1$	1.2 ± 0.3
24912	ξ Per	$+0.3 \pm 0.1$	2.5 ± 0.3	...	...
		$+4.7 \pm 0.5$	3.1 ± 0.5	$+2.0 \pm 0.1$	3.6 ± 0.2
30614	α Cam	$+1.3 \pm 0.8$	4.5 ± 0.9	-0.1 ± 0.2	4.8 ± 0.2
35149	23 Ori	...	...	$+6.5 \pm 0.2$	3.5 ± 0.2
143275	δ Sco	...	...	-2.0 ± 0.3	2.6 ± 0.4
144217 A	β^1 Sco	$+1.9 \pm 0.7$	3.3 ± 0.9	-0.9 ± 0.3	3.2 ± 0.5
144470	ω^1 Sco	$+1.7 \pm 0.6$	3.2 ± 0.7	-1.4 ± 0.2	2.7 ± 0.3
145502	ν Sco AB	$+2.5 \pm 0.5$	2.1 ± 0.7	-0.6 ± 0.4	2.7 ± 0.4
147165	σ Sco	$+3.8 \pm 0.5$	3.1 ± 0.6	$+3.1 \pm 0.6$	2.8 ± 0.7
164353	67 Oph	$+4.2 \pm 0.7$	2.8 ± 0.8	$+2.4 \pm 0.2$	3.2 ± 0.2
167264	15 Sgr	...	...	$+5.9 \pm 0.3$	2.6 ± 0.3
184915	κ Aql	$+1.3 \pm 0.3$	3.0 ± 0.3	$+0.8 \pm 0.3$	2.6 ± 0.3
203064	68 Cyg	$+1.7 \pm 0.5$	4.5 ± 0.6	$+1.8 \pm 0.5$	4.5 ± 0.7
218376	1 Cas	[a]	[a]	-5.7[b]	1.8[b]
		$+1.6 \pm 0.5$	3.2 ± 0.8	$+4.0$[b]	3.9[b]
224572	σ Cas	-8.4 ± 1.1	3.6 ± 1.3	-8.9 ± 0.3	3.5 ± 0.4
		...	...	-15.5 ± 1.1	4.3 ± 1.4

[a] Possible CH feature.
[b] From Hobbs 1973.

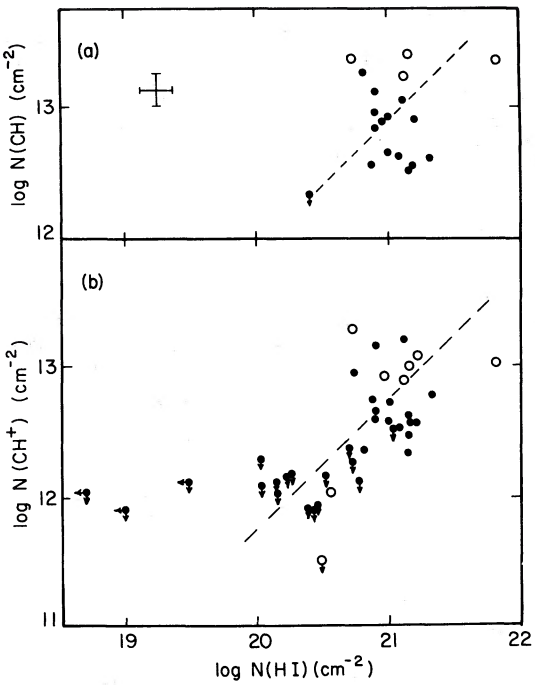

FIG. 1.—(*a*) Log N(CH) plotted against log N(H I); (*b*) log N(CH$^+$) plotted against log N(H I). Filled circles are results reported in the present work; open circles are previous measurements. Limiting values are denoted by arrows. For comparison with chemical models in the text, lines of slope unity are indicated by the dashes. The cross in the upper panel represents typical errors associated with the measurements.

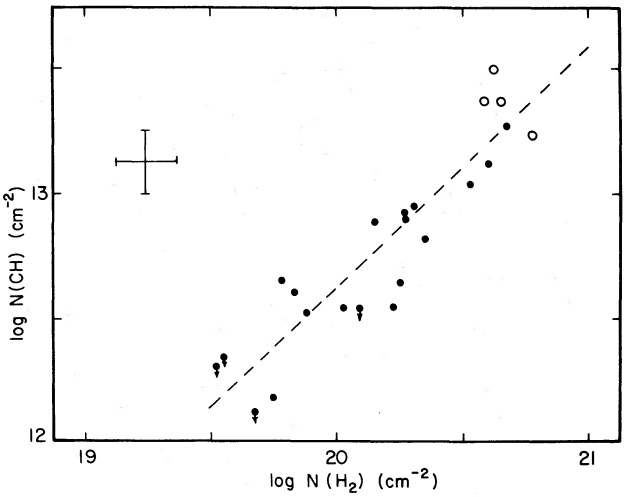

FIG. 2.—N(CH) vs. $N(H_2)$ in a log-log plot. The dashed line is a least-squares fit to the CH detections.

below. No trend in either set of data is apparent; an attempt to find a linear relationship in the data leads to a correlation coefficient, r, less than 0.25 for both plots. The column density of CH versus the column density of H_2 is illustrated in Figure 2; the variation of CH^+ with H_2 is seen in Figure 3. [Since CH did not correlate with H I, but a strong correlation was evident between CH and H_2, the data set for CH was restricted to directions with $N(H_2) \gtrsim 10^{19}$ cm^{-2}. Below this value for $N(H_2)$, detection of CH, if possible, would have required extremely long integrations.] An inspection of Figures 2 and 3 clearly reveals two points: (1) only for directions with $N(H_2) > 10^{19}$ cm^{-2} are there detections of CH and/or CH^+; the one exception is 23 Ori (see below for discussion of this direction), and (2) N(CH) varies linearly with $N(H_2)$ ($r = 0.90$), while only a weak correlation, if any, arises between $N(CH^+)$ and $N(H_2)$ ($r = 0.30$). Last, Figure 4 is a plot of N(CH) against $N(CH^+)$ for the directions which have detectable amounts of both molecules; here a correlation coefficient of 0.20 indicates probable random variation. These results are discussed further in the next section where the data are interpreted in terms of current ideas regarding interstellar molecular chemistry.

III. THEORETICAL INTERPRETATION OF THE DATA

a) Chemistry with Atomic Hydrogen

The reactions important to the chemistry of CH and CH^+ in predominantly atomic gas (Bates and Spitzer

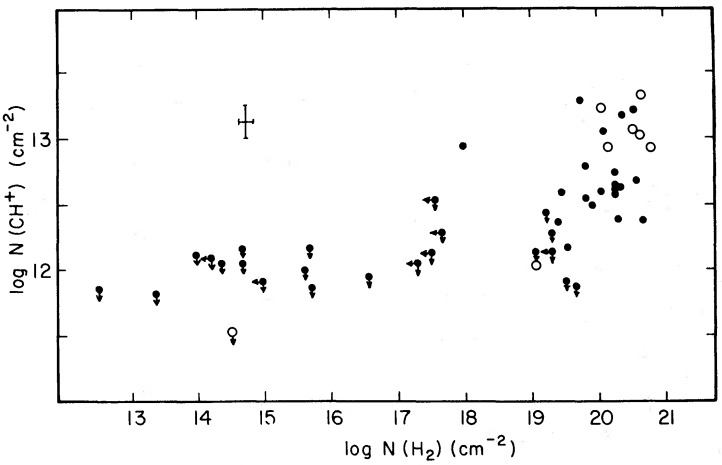

FIG. 3.—A plot of log $N(CH^+)$ vs. log $N(H_2)$

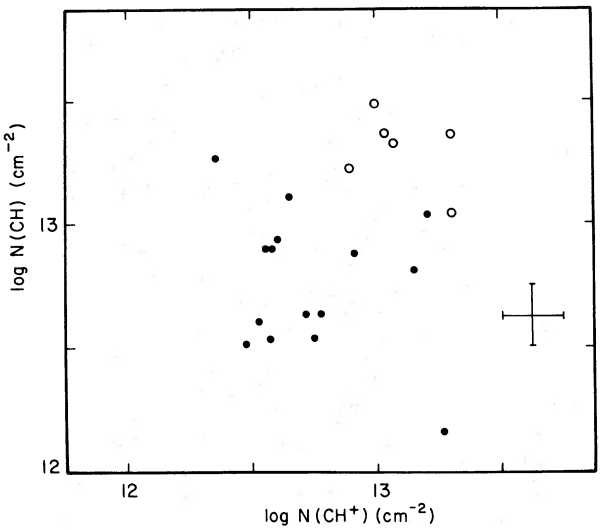

FIG. 4.—A plot of log N(CH) vs. log $N(CH^+)$

1951; Solomon and Klemperer 1972) are found in Table 3. The steady state density of species X, $n(X)$, is obtained by equating production mechanisms with destruction mechanisms:

$$n(\mathrm{CH}) = \frac{k_1 n(\mathrm{C}) n(\mathrm{H\ I})}{G_1 + k_3 n(\mathrm{C}^+)} \quad (1)$$

and

$$n(\mathrm{CH}^+) = \frac{k_2 n(\mathrm{C}^+) n(\mathrm{H\ I})}{k_4 n(\mathrm{e})} . \quad (2)$$

For comparison with observations, global parameters are needed, however. If local parameters do not change appreciably through a cloud, local parameters can be replaced by global ones; then equations (1) and (2) become

$$N(\mathrm{CH}) = \left[\frac{k_1 n(\mathrm{C})}{G_1 + k_3 n(\mathrm{C}^+)}\right] N(\mathrm{H\ I}) \quad (3)$$

and

$$N(\mathrm{CH}^+) = \left[\frac{k_2 n(\mathrm{C}^+)}{k_4 n(\mathrm{e})}\right] N(\mathrm{H\ I}) , \quad (4)$$

TABLE 3

IMPORTANT REACTIONS OCCURRING IN ATOMIC GAS

Reaction	Rate Coefficient (cm^3 s^{-1})
$C + H \rightarrow CH + h\nu$	k_1
$C^+ + H \rightarrow CH^+ + h\nu$	k_2
$CH + h\nu \rightarrow$ all products	G_1/n^a
$CH + C^+ \rightarrow C_2^+ + H$	k_3
$CH^+ + e \rightarrow$ all products	k_4

[a] The photodestruction rate G_1 is expressed in s^{-1}. After dividing by the density n, a parameter with units of a rate coefficient is obtained.

where $N(X) = \int n(X) dr$. The terms in square brackets are independent of n and, therefore, do not affect the relationship between $N(X)$ and N(H I). From equations (3) and (4), both N(CH) and $N(CH^+)$ should vary linearly with N(H I) if the cloud were predominantly atomic gas. Furthermore, N(CH) should be proportional to $N(CH^+)$. With the recently determined rate coefficient for dissociative recombination of CH^+ (Mitchell and McGowen 1978), and with the photodestruction rate for CH of Barsuhn and Nesbit (1978), $N(\mathrm{CH}) \sim 0.03\ N(CH^+)$ in a cloud having a density of 100 cm^{-3} and having a temperature of 80 K. If both molecules are formed in atomic gas, CH would not have been detected!

As can be seen in Figures 1 and 4, the data do not follow the trends expected for chemistry in atomic gas. Both CH and CH^+ should vary linearly with atomic hydrogen, but the data show no such relationship in Figure 1. The data appear randomly scattered about the dashed lines, which have a slope of unity. From Figure 4, no relationship between CH and CH^+ is apparent. One is led to the conclusion that formation of carbon hydrides does not occur in a cloud of primarily atomic gas.

b) *Chemistry in Gas Containing* H_2

Black and Dalgarno (1973) and Black *et al.* studied the chemical network leading toward the formation of CH and CH^+ in a cloud containing molecular hydrogen. A schematic flowchart of the important channels is illustrated in Figure 5. When the various feedback loops are included in the steady state rate equations, the densities for CH and CH^+ become

$$n(\mathrm{CH}) \sim \frac{0.67 k_5 n(\mathrm{C}^+) n(\mathrm{H_2})}{G_1 + k_3 n(\mathrm{C}^+)} \quad (5)$$

$$n(\mathrm{CH}^+) \sim \frac{0.33 k_5 n(\mathrm{C}^+)}{k_6} . \quad (6)$$

If, as before, local densities are assumed constant throughout the cloud and thus represent column densities, N(CH) is predicted to vary linearly with $N(H_2)$, while $N(CH^+)$ is predicted to be independent of H_2. For all lines of sight with molecular hydrogen, $N(CH^+)$ is expected to be a constant fraction of $N(C^+)$. The appropriate reactions are listed in Table 4.

For two specific reasons, the data indicate that both CH and CH^+ form in molecular gas. First, except for

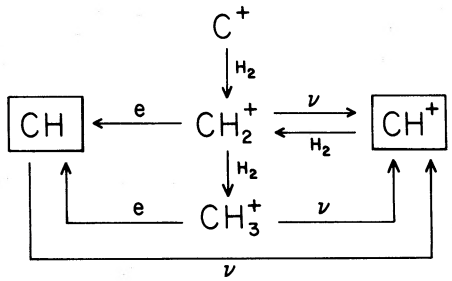

FIG. 5.—The gas phase chemistry for the production of CH and CH^+ in molecular gas.

TABLE 4

IMPORTANT REACTIONS OCCURRING IN MOLECULAR GAS

Reaction	Rate Coefficient ($cm^3\ s^{-1}$)
$CH + C^+ \rightarrow C_2^+ + H$	k_3
$C^+ + H_2 \rightarrow CH_2^+ + h\nu$	k_5
$CH + h\nu \rightarrow C + H$	G_1/n[a]
$CH^+ + H_2 \rightarrow CH_2^+ + H$	k_6

[a] The photodestruction rate G_1 is expressed in s^{-1}. After dividing by the density n, a parameter with units of a rate coefficient is obtained.

23 Ori (which will be discussed in § III*c*), CH and CH^+ are detected only in directions with $N(H_2) > 10^{19}$ cm^{-2}. This column density of H_2 is sufficient to make lines originating from the $J = 0$ and 1 rotational levels of the ground state optically thick. Second, the predictions of the chemical model are borne out by the observations: Namely, $N(CH)$ varies linearly with $N(H_2)$; and $N(CH^+)$ is independent of H_2. A linear least-squares fit to the CH data (detections only) results in the solid curve in Figure 2. The slope of the curve is 1.0 ± 0.1.

Unfortunately, a problem arises if both molecules form in the same parcel of gas. To reproduce the CH data, a value for k_5 of $\sim 5 \times 10^{-16}$ $cm^3\ s^{-1}$ is necessary (Langer 1976; Black and Dalgarno 1977). Such a value is consistent with theoretical estimates for this radiative association (Herbst, Shubert, and Certain 1977; Bates 1978). Since $k_6 \sim 10^{-9}$ $cm^3\ s^{-1}$, the chemical model predicts that $N(CH^+) \sim 10^{-7} N(C^+)$. The estimate for $N(CH^+)$ is two orders of magnitude below the observed results when the results for $N(C^+)$ from *Copernicus* (e.g., Jenkins and Shaya 1979) are used. Though the branching ratios in equations (5) and (6) are similiar, the large difference in column densities for CH and CH^+ arises because in diffuse clouds $k_6 \gg G_1/n(H_2) > k_3$. A larger value for k_5 improves the correspondence between theory and observation for CH^+, but then a discrepancy persists with CH. Elitzur and Watson (1978, 1980) investigated CH^+ formation behind a shock front in an attempt to remove the discrepancy between theory and observation in $N(CH^+)$.

c) Chemistry behind a Shock

Elitzur and Watson proposed the following scenario for the formation of CH and CH^+ in diffuse interstellar clouds. Both molecules are formed behind a shock which is propagating through an atomic cloud. In the high temperature ($\gtrsim 1000$ K) postshock (adiabatic) gas, the reaction

$$C^+ + H_2 \overset{k_3}{\rightleftarrows} CH^+ + H - 0.4\ ev$$

proceeds to the right with a large enough rate to produce observed amounts of CH^+. Approximately one-tenth of the hydrogen atoms are located in the hot postshock gas [i.e., $N(H\ I) \sim 10^{19}$ cm^{-2}]. Molecular fractions, $n(H_2)/[n(H\ I) + 2n(H_2)]$, between 1% and 10% are necessary for CH^+ production. The formation of CH occurs farther downstream in the cooled, compressed postshock (isothermal) gas. Here, the protons primarily are incorporated into hydrogen molecules; the chemistry for producing CH in molecular gas (Black and Dalgarno 1973), therefore, is applicable. Thus, the shock model of Elitzur and Watson also relies on reactions with H_2, but the production channels for CH and CH^+ are independent of each other. This fact removes the problem found in § III*b* involving the production of CH and CH^+ in the same parcel of gas.

The shock model has several observational consequences. Three consequences are chemical in nature. Since CH is produced in the scheme suggested by Black and Dalgarno (1973), equation (5) which shows that $N(CH) \propto N(H_2)$ is appropriate. According to Elitzur and Watson (1978, 1980) and Elitzur (1980), $N(CH^+)$ is expected to be independent of $N(H_2)$. This is illustrated in equation (7):

$$N(CH^+) = n_p v_s \tau x(C^+) x(H_2) E\left(\frac{4700}{T_a}\right) . \qquad (7)$$

Here, n_p is the preshock particle density, v_s is the shock velocity, τ is the cooling time, $x(X)$ is the abundance of species X relative to the total hydrogen content ($H\ I + 2H_2$), T_a is the temperature of the adiabatic gas, and E_1 is the exponential integral of the first kind. Because the cooling of the adiabatic gas occurs through rotational transitions in H_2, the cooling time is inversely proportional to $x(H_2)$. When the relationship between τ and $x(H_2)$ is incorporated into equation (7), no terms involving H_2 remain in the expression for $N(CH^+)$. As discussed in the previous subsection, these trends are found in the data. The inconsistency that arose before no longer applies because the CH and CH^+ are formed via independent chemical networks.

Another observational fact which supports the shock model is that CH absorption occurs only toward directions where CH^+ is detected. As the shock propagates through the gas, CH^+ forms first immediately behind the shock. The CH radical does not form until the postshock gas cools sufficiently and becomes more dense. Several cooling times ($\sim 10^5$ years) have to pass before much production of CH takes place.

Adams (1949) detected CH, but no CH^+, toward 20 Aql and 2 Cyg. The smallest equivalent width that he could measure was about 5 mÅ (Frisch 1972); the present survey includes lines to a limit of ~ 1 mÅ. For several stars in Adams' survey (e.g., the bright stars in Scorpius), he did not detect molecular absorption, but because of the improved limits, absorption was seen in the present work. Unfortunately, hydrogen was not measured toward 20 Aql and 2 Cyg, and, therefore, these stars were not included in the present work. With improved limits, CH^+ absorption with $W_\lambda \sim 1$–5 mÅ probably will be observed toward 20 Aql and 2 Cyg.

The detection of CH^+ toward 23 Ori is no longer an anomaly. For this direction, a shock probably has entered an atomic cloud recently ($t \sim 10^4$ years). There has not been sufficient time for the gas to cool and form an

isothermal region. The observed value for $N(H_2)$ toward 23 Ori is $\sim 10^{18}$ cm^{-2} (Frisch and Jura 1980); such a value is consistent with most, if not all, of the H_2 being in the adiabatic gas.

d) Dynamical Considerations of Shock Chemistry

Though the data conform to the chemical predictions of the shock model, evidence of the dynamics must appear in the data also if this model truly describes the CH and CH^+ measurements. First, a shift in velocity at line center between the lines of CH and CH^+ is expected because each molecule is found in a different part of the fluid flow. In the reference frame of the shock the preshock gas is streaming past the shock at a velocity v_s. In steady state conditions, the conservation of mass across the shock is given by

$$\rho_p v_s = \rho_a v_a \,. \tag{8}$$

The subscripts p and a refer to preshock and adiabatic, respectively. For an adiabatic shock ρ_a equals $4\rho_p$, and v_a is $\frac{1}{4}v_s$. This is the velocity of CH^+. The isothermal gas (where the CH is located) travels at the speed of the shock which is zero in the frame of the shock. The shift between CH and CH^+, therefore, is $\frac{1}{4}v_s$. If a shift in velocity is detected between the lines of CH and CH^+, the shock velocity is known. The sense of the shift determines the direction of the flow. If the CH line is blueshifted (redshifted) relative to the CH^+ line, the flow is moving toward (away from) the Sun. Second, the column density of CH^+ is expected to correlate with the amount of shift seen for lines of sight near each other. In such cases, the other physical parameters are likely to be the same for each line of sight. The abundance, and hence the column density, of CH^+ depends on temperature through the exponential term in the rate coefficient k_7. The exponential temperature term arises because of the endothermicity of the reaction. The temperature behind the shock is related to the velocity of the shock; higher temperatures occur behind faster shocks. The correlation between $N(CH^+)$ and shift is a result of the dependence of the shift on v_s. Third, because the Doppler parameter is also an indication of the temperature, a correlation between $N(CH^+)$ and b is predicted, especially for directions where the second prediction applies. Fourth, the distribution of rotational levels in the ground state of H_2 is likely to be due to collisional excitation occurring behind the shock. The probability of observing such a distribution depends on the efficiency of populating the levels via collisions as opposed to populating them via photon pumping.

The dynamical consequences of the shock model are seen in data taken toward bright stars. Chaffee (1975) found a shift toward ζ Oph; radio observations of other molecules toward ζ Oph (Crutcher 1979; Liszt 1979) indicate emission at the velocity of the CH line, not that of the CH^+ line. In the model of Elitzur and Watson, other molecules form with CH in the isothermal gas. Frisch (1979) noted a shift between the absorption lines of CH and CH^+ toward χ Oph; the shift for this direction was confirmed by the velocity of CH 9 cm emission (Willson 1981). Willson also presented evidence for a shift toward χ^2 Ori and ζ Oph by comparing his data with the optical data for CH^+ (Hobbs 1973). For the lines of sight toward the Perseus OB2 association, Federman (1980) discerned shifts from optical data measured against the continua of o, ζ, and ξ Per. For these nearby lines of sight, two other dynamical aspects of the model were found: $W_\lambda(CH^+)$ correlated with both the shock velocity (through the amount of shift) and the Doppler parameter. The recently detected line of CH toward 20 Tau was shifted from the CH^+ line observed toward this star (Federman 1982). Furthermore, for 20 Tau, as well as nearby 23 and η Tau, the shock makes a major contribution to the distribution H_2 rotational levels. Meyers *et al.* (1982) measured a shift in velocity between CH and CH^+ toward β^1, ω^1, and ν Sco. The results of Federman (1980, 1982) and Meyers *et al.* (1982) are part of the present survey; for a detailed discussion of the results, the reader is referred to the three papers. Here, the lines of sight not previously reported are stressed.

A shift in velocity between the lines of CH and CH^+ can arise in situations which do not require a shock. For example, Black and Dalgarno (1973) suggested that CH forms in the presence of H_2 in the core of a cloud, while CH^+ forms in the outer atomic envelope. The expected correlation between CH^+ and atomic hydrogen, however, is not found in the data presented above; the data indicate that both CH and CH^+ are produced in gas with substantial amounts of H_2. Another possibility is that CH^+ is produced from CH in gas permeated by an enhanced flux of ionizing radiation. The problem here is that CH^+ is reprocessed rapidly into CH through reactions with H_2 (Black and Dalgarno 1973). Thus, CH^+ has to form in a different parcel of molecular gas. The model of Elitzur and Watson (1978, 1980) which incorporates chemistry behind a shock appears the most promising chemical model because (1) the shock model surmounts the difficulties encountered in the steady state models, and (2) additional consequences which are specific to the shock model are found in the data.

IV. INDIVIDUAL LINES OF SIGHT

In this section the results of the present survey are put into perspective by examining the picture that emerges for specific directions. The lines of sight which have detections of both CH and CH^+ are discussed first. The previously published results are omitted here; the reader is referred to the papers by Federman (1980, 1982) and Meyers *et al.* (1982). The section closes with remarks concerning directions where only CH^+ absorption is observed.

a) Stars in Cassiopeia

The directions toward three stars in Cassiopeia, κ Cas, 1 Cas, and σ Cas, show molecular absorption. A problem that arises for each of these directions is the presence of several features. This aggravates the difficulty in assigning a specific CH feature to a specific CH^+ feature. Toward σ Cas, for example, CH absorption is found at $+1.6$ km s^{-1}, while Hobbs (1973) found CH^+ absorption

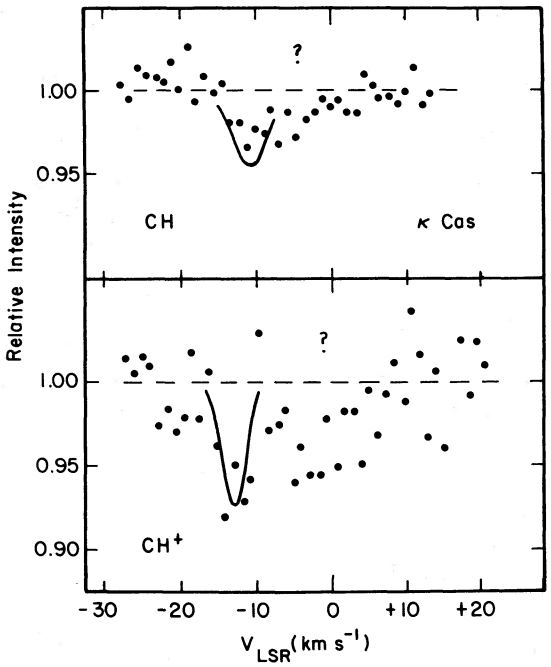

FIG. 6.—Molecular spectra toward κ Cas—(*a*) CH spectrum; (*b*) CH^+ spectrum. The abscissa is the velocity in the local standard of rest. The dashed line is the adopted continuum, while the solid curve is a least-squares Gaussian fit to the absorption line. The question mark indicates a possible feature.

at +4.0 km s^{-1}. One cannot state with confidence that a shift exists, because the CH^+ line is much broader than other CH^+ lines in the work of Hobbs (1973). Most likely, the CH^+ line is a blend of two components, with one of the components having nearly the same velocity as the CH line.

A shift in velocity between the lines of CH and CH^+, at the 2 σ limit, is seen toward κ Cas. The spectra are shown in Figure 6. The CH line is redshifted by 2.0 $\pm$ 0.9 km s^{-1} relative to the CH^+ line. Because the CH is redshifted, the shock is moving at a velocity of $\sim$10 km s^{-1} away from the Sun. The reason for the shock is uncertain because the line of sight toward this star passes through a kiloparsec of interstellar space. There is no clear way to determine the location of the molecular gas with respect to the star. The one piece of information available is that the radial velocity of the star is $\sim$10 km s^{-1} redward of the molecular velocities.

No shifts are discernable toward 1 Cas and σ Cas. This fact is partly due to the difficulty mentioned above in relating specific components to one another. The data for σ Cas are displayed in Figure 7. There are two components in CH^+; the CH absorption probably corresponds to the redder component (-8.9 km s^{-1}). A 2 σ upper limit for a shift is 2.8 km s^{-1}. Most of the uncertainty arises from the placement of the CH line.

b) *Other Directions with* CH *and* CH^+ *Absorption*

Both molecules are found toward α Cam, 67 Oph, κ Aql, and 68 Cyg. A shift between CH and CH^+ may be present toward 67 Oph, but for the other directions, 2 σ upper limits for a shift range from 1.2 to 2.0 km s^{-1}. The possible shift toward 67 Oph is 1.8 $\pm$ 0.9 km s^{-1} ($v_s \sim 8$ km s^{-1}). Figure 8 shows the data toward 67 Oph. The two strongest Ca II features observed by Marschall and Hobbs (1972) correspond in velocity to the two molecular components. The CH line is redshifted from the CH^+ line, indicating flow away from the Sun. 67 Oph is $\sim$30° in galactic longitude from the Sco OB2 association. Thus, though the CH also is redshifted toward stars in the association, the explanation for the flow toward 67 Oph cannot be the same as the explanation for the flow toward the association (Meyers *et al.* 1982). The cause of the flow is unknown.

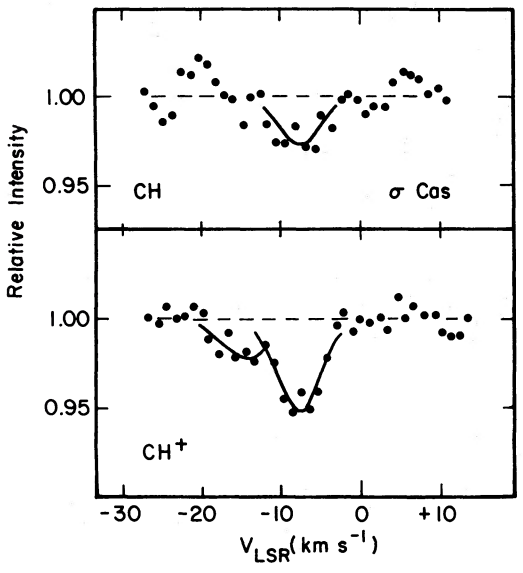

FIG. 7.—Same as Fig. 6 for measurements toward σ Cas

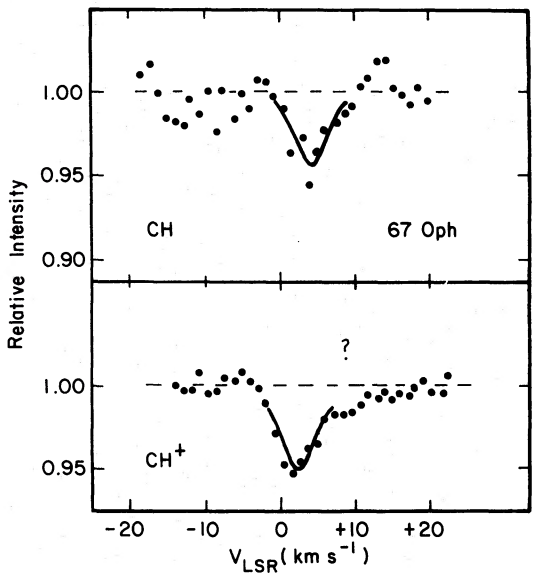

FIG. 8.—Same as Fig. 6 for measurements toward 67 Oph

c) Directions with only CH^+ Detections

The column density of CH correlates well with $N(H_2)$ for directions with $N(H_2) > 10^{19}$ cm^{-2}. As Figure 2 illustrates, CH measurements with $W_\lambda \lesssim 1$ mÅ [$N(CH) \lesssim 10^{12}$ cm^{-2}] occur for directions with $N(H_2) \lesssim 6 \times 10^{19}$ cm^{-2}. Since the lines of sight toward HD 21278, 23 Ori, and δ Sco each have $N(H_2)$ less than 6×10^{19} cm^{-2}, a search for CH absorption was not made. Integration times would have been excessive. No useful limit was possible for 15 Sgr, which has sufficient H_2 along the line of sight, because of poor observing conditions.

Both directions toward δ Sco and 15 Sgr have CH^+ lines which agree in velocity and width with CH^+ lines toward other nearby stars. For δ Sco, the CH^+ line is consistent with other data toward the Sco OB2 association. From the observed distribution of H_2 rotational levels (Spitzer, Cochran, and Hirshfeld 1974), an upper limit for the shock velocity is 10 km s^{-1}. This is the velocity found for the other directions in the association (Meyers *et al.* 1982). The CH^+ line detected in the line of sight toward 15 Sgr has velocity and width similar to the CH^+ line detected by Hobbs (1973) for the nearby line of sight toward μ Sgr. No trend between W_λ and either v_s or b is apparent in data toward either Scorpius or Sagittarius because the values for W_λ, v_s, and b are similar for nearby directions.

The results for 23 Ori suggest a shock recently entered the cloud, thus explaining the smaller amount of H_2 seen toward the star. Frisch and Jura (1980) noted that the even-J and odd-J rotational ladders are described best by separate Doppler parameters. The odd-J ladder has the larger value for b. From a statistical point of view, the odd-J ladder is expected to represent a larger fraction of the total amount of H_2 for temperatures above $\sim$100 K. The large b-value for the odd-J ladder may arise because hot postshock and cooling postshock gas contributes to the column densities, while only cooling gas contributes to the column densities for the even-J rotational levels. A shock velocity of $\sim$15 km s^{-1} can make a substantial contribution to the observed distribution of odd-J rotational levels.

V. CONCLUSIONS

From an extensive set of measurements, specific conclusions concerning the gas phase chemistry of CH and CH^+ can be stated with more confidence than was possible previously. Neither molecule is formed in predominantly atomic gas. The production of CH and CH^+ occurs through reactions involving molecular hydrogen because the radicals are observed only toward directions with substantial amounts of H_2. Different parcels of gas are needed to explain the observed amounts of both CH and CH^+. The most consistent chemical model includes the presence of a shock. In this model, CH^+ is formed in the hot postshock gas, and CH is formed in the compressed, cooled postshock gas.

Dynamical aspects of the shock model also are seen in the data. For approximately 50% of the directions with detections of both CH and CH^+, the line of CH is shifted in velocity from that of CH^+. The separation in velocity is typically 2–3 km s^{-1}. These results are displayed in Figure 9, where 2 σ limits about $\Delta v = v_{CH} - v_{CH^+}$ are shown. If a measurement crosses the dashed line representing $\Delta v = 0$ km s^{-1}, only an upper limit can be deduced. The preponderance of redshifts is understood easily when one realizes that the directions toward stars in Perseus and Scorpius account for most of the redshifts in the present, limited survey. Shocks probably exist along the remaining lines of sight, but geometrical factors and observational limitations hinder the detection of the shocks.

Two points regarding the observed correlation between CH and H_2 require attention. First, such a correlation is consistent with the suggestion of Federman *et al.* (1980) that molecules such as CH, CO, and H_2 occupy the same volume of space. Protection from the interstellar ultraviolet radiation field is necessary for each of these molecules. Second, the correlation found from the present survey is consistent with the correspondence between N(CH) and A_B found for dark clouds (see Sandell *et al.* 1981), indicating that the gas phase chemical network occurring in diffuse clouds ($A_v \lesssim 1$ mag) also is appropriate for dark clouds ($A_v \lesssim 4$ mag). For the diffuse clouds studied here, N(CH) is approximately 10^{13} cm^{-2} for a cloud with $N(H_2) \sim 3 \times 10^{20}$ cm^{-2}. If half the gas is molecular, then $N(H\,I + 2H_2) \sim 10^{21}$ cm^{-2}. The total column density of protons is equivalent to 0.5 mag of visible extinction (Bohlin *et al.*). The column density of CH then is given by 2×10^{13} (A_v/mag) cm^{-2}. The result of averaging the data presented in Sandell *et al.* is $N(CH) \sim 3 \times 10^{13} (A_B/\text{mag})\text{cm}^{-2}$ or $N(CH) \sim 2 \times 10^{13}$ (A_v/mag) cm^{-2}.

The similarity in the results for diffuse and dark clouds is anticipated in equation (5). When dark clouds are searched for CH emission, only the outer portion of

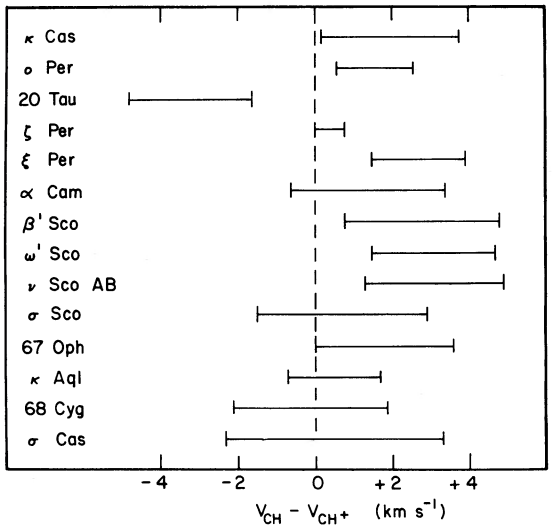

FIG. 9.—Representation of the amount of shift in velocity between the lines of CH and CH^+. 2 σ limits about the observed shift are shown.

the cloud is sampled because the collisional excitation responsible for 9 cm emission occurs at low densities ($n \gtrsim 30$ cm^{-3}). Both optical and radio measurements of CH then refer to the outer portions of a dark cloud, though the radio measurements probably are somewhat farther into the cloud ($A_v \lesssim 4$ mag compared to $A_v \lesssim 1$ mag). The applicability of equation (5) results from the fact that the cloud envelope is likely to have most of the carbon in the form of C^+. Furthermore, for both types of clouds N(CH) is expected to vary linearly with $N(H_2)$. In diffuse clouds $N(C^+)$ depends weakly on $N(H_2)$ because of the large amount of neutral hydrogen present. When A_v approaches 4 mag in dark clouds, $N(H_2)$ is substantially greater than N(H I), and $N(C^+)$ becomes proportional to $N(H_2)$. Thus, if either photodestruction (as in diffuse clouds) or destruction through collisional reactions (as in the most reddened dark clouds) occurs, the dependence of N(CH) on $N(H_2)$ is not altered.

A clearer picture of molecular chemistry in diffuse interstellar clouds is emerging. Molecules which incorporate heavy nuclei are found in regions containing molecular hydrogen. When a shock passes through an atomic cloud, an increase in the abundance of H_2 occurs behind the shock. Immediately behind the shock, CH^+ forms. Farther downstream in the compressed gas is where molecules like CH and CO form. The observed value of N(CH)/N(CO) is $\sim$0.05–0.10; the upper limits found here for CH toward o And and ϵ Per are consistent with this ratio when the results for CO of Federman *et al.* are considered. Since the diffuse cloud chemistry for both CH and CO (Federman *et al.*) seems applicable to dark clouds, the regions of CH and CO absorption may be the outer edges of dark clouds. Additional optical and radio measurements are needed to substantiate this suggestion. The number of directions where other molecules (CN, OH, C_2) have been detected is very limited; more data on the other molecules are required before chemical trends can be quantified. Though shock chemistry is not necessary for the production of molecules other than CH^+, shocks are commonplace because CH^+ is observed toward most of the directions where CO is seen in absorption and toward all the directions where CH is seen in absorption.

This research was supported through grant F-623 of the Robert A. Welch Foundation.

REFERENCES

Adams, W. S. 1949, *Ap. J.*, **109**, 354.
Barsuhn, J., and Nesbit, R. K. 1978, *J. Chem. Phys.*, **68**, 2783.
Bates, D. R. 1978, *Proc. Roy. Soc. London, A*, **360**, 1.
Bates, D. R., and Spitzer, L. 1951, *Ap. J.*, **113**, 441.
Black, J. H., and Dalgarno, A. 1973, *Ap. Letters*, **15**, 79.
———. 1977, *Ap. J. Suppl.*, **34**, 405.
Black, J. H., Dalgarno, A., and Oppenheimer, M. 1975, *Ap. J.*, **199**, 633.
Bohlin, R. C., Savage, B. D., and Drake, J. F. 1978, *Ap. J.*, **224**, 132.
Brzozowski, J., Bunker, P., Elander, N., and Erman, P. 1976, *Ap. J.*, **207**, 414.
Chaffee, F. H. 1974, *Ap. J.*, **189**, 427.
———. 1975, *Ap. J.*, **199**, 379.
Chaffee, F. H., and Dunham, T. 1979, *Ap. J.*, **233**, 568.
Cohen, J. G. 1973, *Ap. J.*, **186**, 149.
Crutcher, R. M. 1979, *Ap. J.* (*Letters*), **231**, L151.
Elitzer, M. 1980, *Astr. Ap.*, **81**, 351.
Elitzer, M., and Watson, W. D. 1978, *Ap. J.* (*Letters*), **222**, L141.
———. 1980, *Ap. J.*, **236**, 172.
Erman, P. 1977, *Ap. J.* (*Letters*), **213**, L89.
Federman, S. R. 1980, *Ap. J.* (*Letters*), **241**, L109.
———. 1982, *Ap. J.*, in press.
Federman, S. R., Glassgold, A. E., Jenkins, E. B., and Shays, E. J. 1980, *Ap. J.*, **242**, 545.
Fink, E. H., and Welge, K. H. 1967, *J. Chem. Phys.*, **46**, 4315.
Frisch, P. 1972, *Ap. J.*, **173**, 301.
———. 1979, *Ap. J.*, **227**, 474.
Frisch, P. C., and Jura, M. 1980, *Ap. J.*, **242**, 560.
Herbst, E., Shubert, J. G., and Certain, P. R. 1977, *Ap. J.*, **213**, 696.
Hesser, J. E., and Lutz, B. L. 1970, *Ap. J.*, **159**, 703.
Hobbs, L. M. 1973, *Ap. J.*, **181**, 79.
Jenkins, E. B., and Shaya, E. J. 1979, *Ap. J.*, **231**, 55.
Jura, M., and Smith, W. H. 1977, *Ap. J.*, **215**, 517.
Langer, W. D. 1976, *Ap. J.*, **206**, 699.
Linevsky, M. J. 1967, *J. Chem. Phys.*, **47**, 3485.
Liszt, H. S. 1979, *Ap. J.* (*Letters*), **233**, L147.
Mahan, B. H., and O'Keefe, A. 1981, *Ap. J.*, **248**, 1209.
Marschall, L. A., and Hobbs, L. M. 1972, *Ap. J.*, **173**, 43.
Meyers, K. A., Snow, T. P., Federman, S. R., and Breger, M. 1982, in preparation.
Mitchell, J. B., and McGowen, J. W. 1978, *Ap. J.* (*Letters*), **222**, L77.
Sandell, G., Johansson, L. E. B., Nguyen-Q-Rieu, and Mattila, K. 1981, *Astr. Ap.*, **97**, 317.
Savage, B. D., Bohlin, R. C., Drake, J. F., and Budich, W. 1977, *Ap. J.*, **216**, 291.
Solomon, P. M., and Klemperer, W. 1972, *Ap. J.*, **178**, 389.
Spitzer, L., Cochran, W. D., and Hirshfeld, A. 1974, *Ap. J. Suppl.*, **28**, 373.
Vogt, S. S., Tull, R. G., and Kelton, P. 1978, *Appl. Optics*, **17**, 574.
Willson, R. F. 1981, *Ap. J.*, **247**. 116.

S. R. FEDERMAN: Department of Astronomy, University of Texas, Austin, TX 78712